Supplementary Materials for

Chip-scale nonlinear bandwidth enhancement via birefringent mode hybridization

Tingge Yuan[a,†], Jiangwei Wu[a,†], Xueyi Wang[a], Chengyu chen[a], Hao Li[a], Bo Wang[a], Yuping Chen[a,*], Xianfeng Chen[a,b]

[a] State Key Laboratory of Advanced Optical Communication Systems and Networks, School of Physics and Astronomy, Shanghai Jiao Tong University, 800 Dongchuan Road, Shanghai 200240, China

[b] Collaborative Innovation Center of Light Manipulations and Applications, Shandong Normal University, Jinan 250358, China

[†] These authors contributed equally to this work

1. Theoretical analysis of the broadband SHG in a first-order SQPM waveguide

In our experiment, broadband frequency conversion was also observed in a first-order SQPM bent waveguide with a radius of 75 μm and a straight waveguide length L_0 of about 2.2 μm, corresponding to the coherent length of the SHG at the FW wavelength around 1550 nm. In this document, we will provide more theoretical details of the QGVM to explain the broadband nonlinear phenomenon in this structure.

In practice, it is difficult to achieve 100 percent intermodal conversion efficiency through the mode hybridization, which means as the SH light propagates through the hybridization point, part of the energy will still exist in the TE0 mode as shown in Fig.s1(a). Therefore, hybridization between the fundamental TE and TM modes may occur at $\theta = \pm 26°$. Considering this hybridization process, we have calculated the corresponding vector-mismatch dispersion $\mathrm{d}k_2(\theta)/\mathrm{d}\lambda$ and its average value $\mathrm{d}k_2'/\mathrm{d}\lambda$ in Fig.s1(a) and (b). Different from the hybrid mode we selected in the main text, here both the first-order and second-order dispersion of the average vector-mismatch in the half-circle waveguide is much closer to 0 so that QGVM can only be realized when the circumference of the half-circle waveguide is much larger than the length of the straight waveguide.

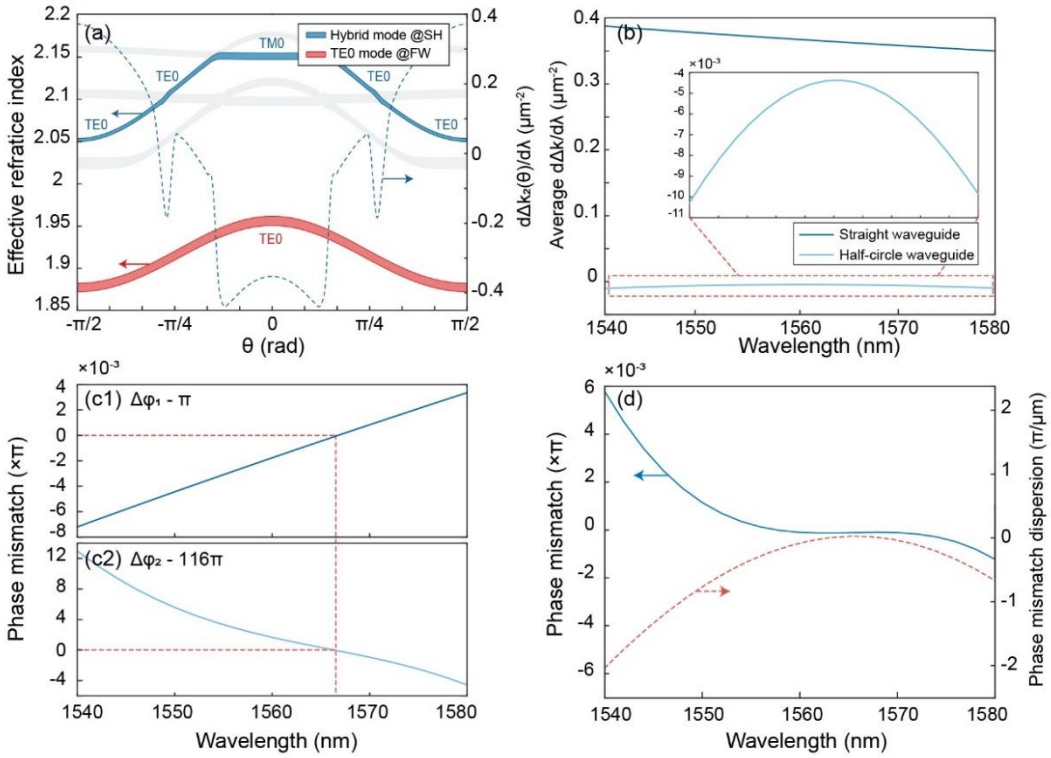

Fig.s1. (a) Effective refractive indexes of the hybrid mode at the SH band and TE0 mode at the FW band in the half-circle waveguide, and corresponding vector mismatch between them. (b) Average vector-mismatch dispersion versus different FW wavelengths, which is positive in the straight waveguide and negative in the half-circle waveguide. (c) Calculated phase mismatch $\Delta\phi_1$ in the straight waveguide and phase mismatch $\Delta\phi_2$ in the half-circle waveguide of a first-order perfect SQPM bent waveguide. (d) Summation of the phase-mismatch represented by $\Delta\phi_1 + \Delta\phi_2 - 117\pi$ with the blue curve, and its first-order dispersion $\mathrm{d}(\Delta\phi_1 + \Delta\phi_2)/\mathrm{d}\lambda$ with the dashed red curve.

The dispersion property of the phase-mismatch in the bent waveguide is calculated in Fig.s1(c), from which we can see that perfect first-order SQPM is realized around the FW wavelength of 1562 nm, and the zero-point of phase-mismatch dispersion $\mathrm{d}(\Delta\varphi_1 + \Delta\varphi_2)/\mathrm{d}\lambda$ is also achieved around this wavelength at the room temperature. And this is why we can use this structure to realize the broadband frequency conversion.

Furthermore, we have numerically calculated the dependence of the SHG bandwidth on the period number N in Fig.s2. As N increases, conversion efficiency grows quadratically with it, and the bandwidth will rapidly decrease from hundreds of nanometers at first and tends to be stable for a longer propagation distance. In our fabricated structure $N = 50$, the predicted 3-dB bandwidth is about 48 nm, as the SH

spectrum illustrated in the inset of Fig.s2, while the measured pump bandwidth in our experiment is about 16nm, which is most limited by the bandwidth of the pump light source.

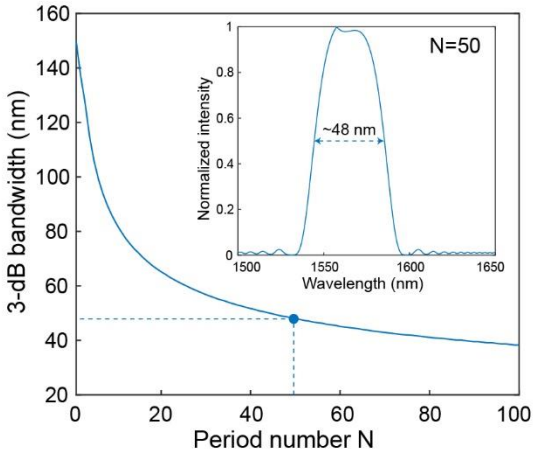

Fig.s2. Theoretical prediction of the 3-dB bandwidth of the SHG in a first-order SQPM waveguide versus different period number N. Inset: simulated SH spectrum at $N = 50$.

2. Theoretically predicted 3-dB SHG bandwidth in perfect and phase-compensated SQPM waveguides

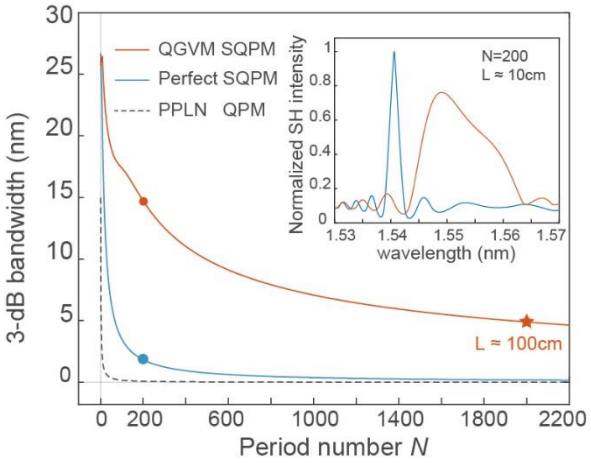

Fig.s3. (b) Calculated SHG bandwidth by QGVM SQPM, perfect SQPM, and PPLN-based QPM, which are about 15 nm, 1.8 nm, and 0.08 nm at N = 200, respectively.

In this section, we show that the geometric parameters of the 111th order phase-compensated SQPM racetrack resonator proposed in the main text can also be used for the broadband SHG in the bent-waveguide configuration, and the differences with the perfect SQPM are shown as well. The numerically calculated SHG 3-dB bandwidths are plotted in Fig versus the different period number N. Even if N increases to 2000,

corresponding to a bent-waveguide with a total length of 100 cm, the SH bandwidth with QGVM is about 5 nm, which is approximately one or two orders of magnitude larger in comparison to the perfect SQPM and PPPLN-based QPM at the same SH output. As the total length of the waveguide increases to 1 m (N~2000), the 3-dB QGVM bandwidth remains relatively stable with a value larger than 5 nm, which suggests the huge potential of QGVM in ultra-long-distance nonlinear frequency conversion.

3. Improvement of the conversion efficiency in a SQPM racetrack resonator

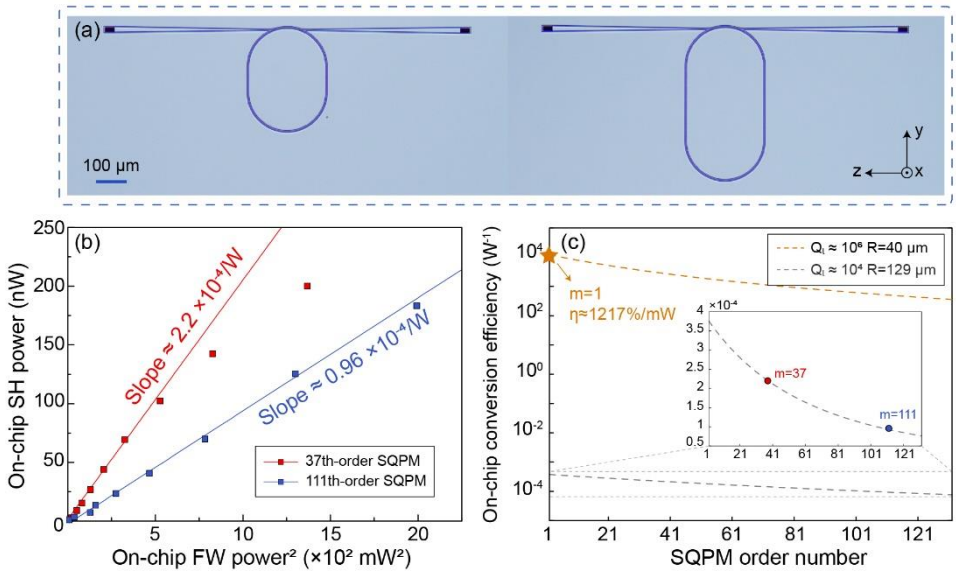

Fig.s4. (a) Optical-microscopic images of the fabricated 37th and 111th-order SQPM racetrack resonators, and (b) corresponding on-chip SHG conversion efficiencies. (b) Theoretical prediction of the conversion efficiencies for different SQPM order numbers in the experimentally fabricated structure (Q≈ 10^4, R≈129μm), and an improved structure (Q≈ 10^6, R≈40μm).

In our experiment, the conversion efficiency of the broadband SHG in the 111th-order SQPM racetrack resonator is mainly limited by the Q-factor and the relatively large size (SQPM order) of the racetrack resonator, and their effects on the conversion efficiency can be roughly summarized as

$$\eta \propto \frac{Q^3}{(2\pi R + 2L_0)^3}. \qquad (s1)$$

Thus, lowering the SQPM order number m, decreasing the half-circle radius R, and

improving the Q factor can efficiently enhance the conversion efficiency. We have performed another SHG experiment in a perfect 37th ($L_0 = 81.2\ \mu$m) and 111th-order ($L_0 = 245.4\ \mu$m) SQPM racetrack resonators, which have the same design in terms of the radius, waveguide width, and coupling structure, with a close Q factor of about 10^4. Fig.s4(a) shows their on-chip conversion efficiencies, where the normalized efficiency has been increased to about twice as the SQPM order number decreases from 111 to 37.

A detailed theoretical analysis of the on-chip conversion efficiency can be found in our previous work (Ref. 42 in the manuscript), based on which the theoretically predicted conversion efficiency for different SQPM order numbers in our fabricated structure is shown in Fig.r1(b), which is in good agreement with our experimental results. For an optimized structure with a smaller radius of 40 μm and an improved Q factor of about 10^6, the theoretically predicted on-chip conversion efficiency can reach the order of 10^5 %/W for an SQPM order number lower than 50, which is sufficient for the quantum applications, and expected to be realized if the fabrication process can be optimized.